

Support Information

Equilibrating bonding energy between solvent and solute for optimized crystallization enables efficient perovskite solar cells

Hanzhi Zhang^{a#}, Weihui Bi^{a#}, Jin Wang^{b*}, Peng Mao^b, Jun Lv^{b,c}, Shen Xing^d, Po-Chuan Yang^e, Guangtong Hai^f, Gaorong Han^a, Yufei Zhong^{b*}

^a Zhejiang engineering research center for fabrication and application of advanced photovoltaic materials, Institute for Carbon Neutrality, Ningbo Innovation Centre, Zhejiang University, Ningbo, 315048, P. R. China.

^b Zhejiang engineering research center for fabrication and application of advanced photovoltaic materials, School of Materials Science and Engineering, NingboTech University, No.1 Qianhu South Road, Ningbo, 315100, P. R. China.

^c School of Material Science and Engineering, Zhejiang University, Zheda Road 38, Hangzhou, 310027, P. R. China.

^d Nanjing University, Nanjing, Jiangsu 210008, P. R. China.

^e Dresden Integrated Center for Applied Physics and Photonic Materials (IAPP) and Institute of Applied Physics, TU Dresden, Nöthnitzer Str. 61, 01187 Dresden, GermanyRISEN Energy Co., Ltd.

^f College of Chemical and Biological Engineering, Zhejiang University, Hangzhou 310027, China.

[#] Hanzhi Zhang and Weihui Bi contributed equally to this work.

*Corresponding Author

E-mail address:

wjin@nit.zju.edu.cn, yufei.zhong@nit.zju.edu.cn

Experimental

Materials

Formamidinium iodide (FAI), lead iodide (PbI_2), methylamine hydrochloride (MAH), methylammonium bromide (MABr), lead bromide (PbBr_2), cesium iodide (CsI), bathocuproine (BCP), phenyl-C₆₁-butyric acid methyl ester (PCBM) and 2-Phenylethylamine Hydroiodide (PEAI) are purchased from Xi'an Polymer Light Technology Corp. Anhydrous isopropanol (IPA), N,N-dimethylformamide (DMF) and dimethyl sulfoxide (DMSO), Chlorobenzene (CB) and 2-Methoxyethanol (2-ME) are purchased from Sigma Aldrich. The δ -valerolactone (GVL) are purchased from Aladdin. [4-(3,6-dimethyl-9H-carbazol-9-yl) butyl] phosphonic acid (Me-4PACz) patterned ITO-coated substrates (sheet resistance: 15 ohms/square) are purchased from You Xuan Technology Limited. The above materials are used directly without further purification.

Sample preparation

In this work, the perovskite layer in p-i-n structured PSCs was prepared by one-step reverse solvent method. The physical structure of the device is ITO/SAMs/(FAPbI₃)_{0.95}(MAPbBr₃)_{0.05}/PEAI/PCBM/BCP/Ag.

Fabrication of 12.5% GVL:

The ITO glass substrates (2cm × 2cm) are ultrasonic cleaned with isopropanol for 30 minutes, then dried with nitrogen, and cleaned in plasma for 30 minutes. The as-prepared substrates are exposed to a UV ozone cleaner for 30 min before HTL deposition. The following operations are done in the N₂ atmosphere glove box. Me-4PACz dissolves in 2-Methoxyethanol to prepare HTL solution with a concentration of 1 mg/ml. HTL is coated by spin-coating from the HTL solution at a speed of 5000 rpm for 30 s. Subsequently, the HTL coated substrates are annealed at 100 °C for 10 min. Preparation of perovskite precursor solution: 1.276 mmol of FAI, 1.405 mmol of PbCl_2 and 0.255 mmol of MAH, 0.067 mmol of MABr, 0.074 mmol of PbBr_2 , 0.069 mmol of CsI dissolve in the mixture of 0.768ml anhydrous DMF, 0.232ml DMSO and 0.125ml GVL. The perovskite precursor solution is coated onto the ITO/SAMs substrate by two consecutive spin-coating steps, at 1000 and 5000 rpm for 10 s and 30 s, respectively. During the second spin-coating step, 120 μL CB is poured onto the

substrate at the last 5s. Then, the resultant substrate is annealed at 100 °C for 30 min. PEAI (2 mg) is dissolved in isopropyl (1mL) alcohol forming a homogeneous solution, which is spin-coated at 2000 rpm/s for 30 s on ITO/SAMs/(FAPbI₃)_{0.95}(MAPbBr₃)_{0.05} substrate. It is then placed on a hot table and annealed at 100 °C for 5 min to evaporate the solvent. PCBM was dissolved in chlorobenzene with a concentration of 20 mg/mL. ETL is deposited by spin-coating from PCBM solution at 1500 rpm/s for 60 s on ITO/SAMs/(FAPbI₃)_{0.95}(MAPbBr₃)_{0.05}/PEAI substrate. BCP/isopropyl alcohol solution with a concentration of 0.5 mg/mL is coated at a speed of 4500 rpm for 30 s on ITO/SAMs/(FAPbI₃)_{0.95}(MAPbBr₃)_{0.05}/PEAI/PCBM substrate. Finally, 80 nm Ag film is deposited as counter electrode by thermal evaporation. According to the specifications of the mask plate, the effective area of all devices is 0.0386 cm².

Fabrication of 0% GVL:

Except that no GVL was added to the precursor solution, the other steps were consistent with the preparation of 12.5% GVL.

Fabrication of 14.3% GVL:

The preparation method of 14.3%GVL is the same as that of 12.5% GVL, except that the composition of solvent in perovskite precursor solution is different. The preparation of perovskite precursor solution for 14.3% GVL:1.276 mmol of FAI, 1.405 mmol of PbCl₂ and 0.255 mmol of MAcl, 0.067 mmol of MABr, 0.074 mmol of PbBr₂, 0.069 mmol of CsI dissolve in the mixture of 0.768 ml anhydrous DMF, 0.232 ml DMSO and 0.143 ml GVL.

Fabrication of 11.1% GVL:

The preparation method of 11.1%GVL is the same as that of 12.5% GVL, except that the composition of solvent in perovskite precursor solution is different. The preparation of perovskite precursor solution for 11.1% GVL:1.276 mmol of FAI, 1.405 mmol of PbCl₂ and 0.255 mmol of MAcl, 0.067 mmol of MABr, 0.074 mmol of PbBr₂, 0.069 mmol of CsI dissolve in the mixture of 0.768 ml anhydrous DMF, 0.232 ml DMSO and 0.111 ml GVL.

Characterization

FTIR spectroscopy spectra were recorded by Thermo Scientific Nicolet iS5. XRD characterization was performed on a RegakuD/Max-2500 diffractometer equipped using a Cu κ 1 radiation ($\lambda = 1.54056 \text{ \AA}$). The surface morphology and cross-sectional images of samples were observed by a field emission SEM (FEI QUANTA 3D FESEM). UV-vis spectra of perovskite films were obtained from a Lambda 950 UV-vis spectrophotometer. The absorption spectra of perovskite precursor solution were measured by a UV-vis spectrophotometer (UH4150, Hitachi). The EQE of the devices was measured using the ORIEL ique-200 measuring system. Steady-state PL spectrum was measured using a LabRAM HR800 (Horiba Jobin Yvon) equipped with a laser, and the excitation source wavelength is 532 nm. TRPL measurements were conducted by a fluorescence spectrometer with an excitation wavelength of 485 nm (DeltaFlex, Horiba). The TPV and transient photocurrent were conducted multi-function carrier mobility measurement system (PAIOS) with a microsecond pulse white light source (15.2 mW/cm^2). J - V performance measurements of devices under standard AM 1.5G simulated sunlight with a source meter (Keithley 2420), and the simulated light intensity (100 mW/cm^2) was calibrated with a reference silicon solar cell. The step meter - surface profile meter (Dektak -XT 10th) was used to measure the thickness of the films. The Keysight Technologies 7500 (AFM) was used to obtain surface RMS roughness of perovskite films and the scan area is $5 \text{ }\mu\text{m}$. The devices were analyzed in a frequency range from 1 MHz to 10 MHz using Zahner electrochemical workstation. The Keysight Technologies 7500 (KPFM) was used to obtain Surface potential difference of perovskite films and the scan area is $100 \text{ }\mu\text{m}^2$. In situ-PL measurements were conducted by on-line in-situ fluorescence spectrometer with ultraviolet excitation source.

DFT calculation

All the density-functional theory (DFT) computations were performed using the Gaussian 16 Software Package.¹ The 6-311G(d,p) basis set was employed to expand the wave functions.² For the electron-electron exchange and correlation interactions, the functional B3LYP, a form of the hybrid functional, was used throughout.³ The vander-Waals interaction was described using the DFT-D3BJ method that proposed by Grimme.⁴

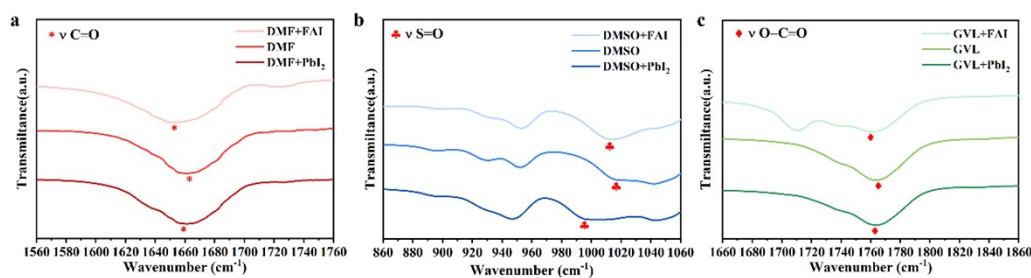


Fig S1. FTIR spectra of (a) DMF, (b) DMSO, (c) GVL, DMF/DMSO/GVL solution of FAI and DMF/DMSO/GVL solution of PbI₂.

As shown in Figure S1a, the carbonyl absorption peak located at 1661 cm⁻¹ undergoes a blue shift after dissolution of PbI₂ and FAI. The similar results present in Figure S1b-c. The absorption peak of sulfonyl (1016 cm⁻¹) provides a most significant shift for DMSO solution of PbI₂, illuminating the most interaction between DMSO and PbI₂. The absorption peak of ester group within GVL (1763 cm⁻¹) affords little shift caused by low solubility and weak interaction between GVL and PbI₂. However, GVL solution of FAI exhibits a more obvious blue shift for the absorption peak of ester group, clarifying the relative strong interaction between FAI and GVL.

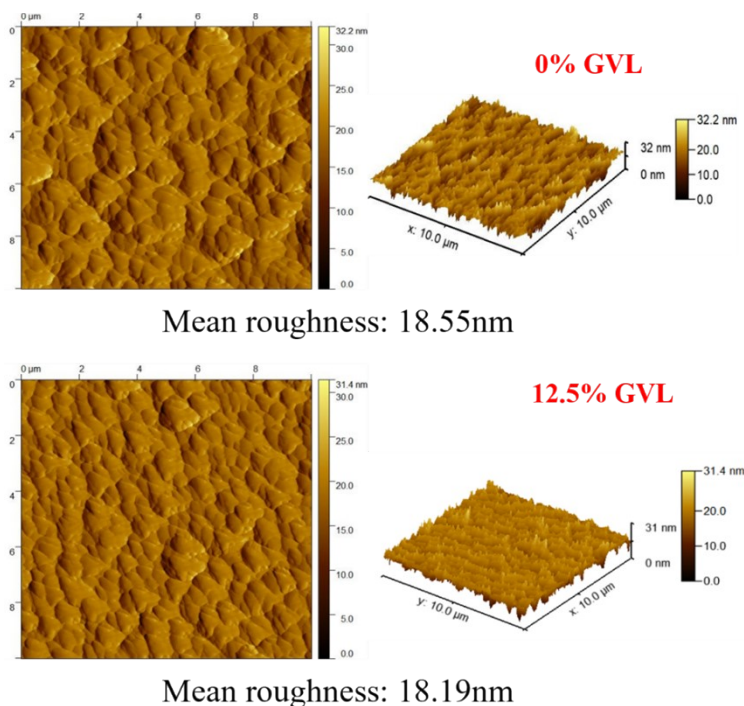


Fig. S2 Atomic force microscope (AFM) images of 0% GVL and 12.5% GVL based perovskite films.

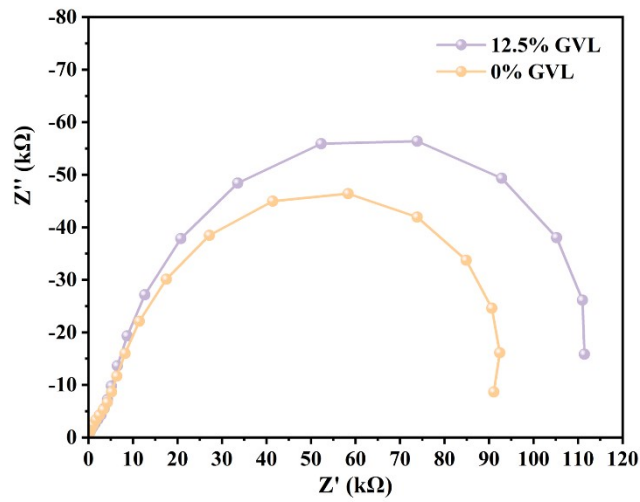


Fig. S3 Electrochemical impedance spectroscopy of 0% GVL and 12.5% GVL devices measured in the dark.

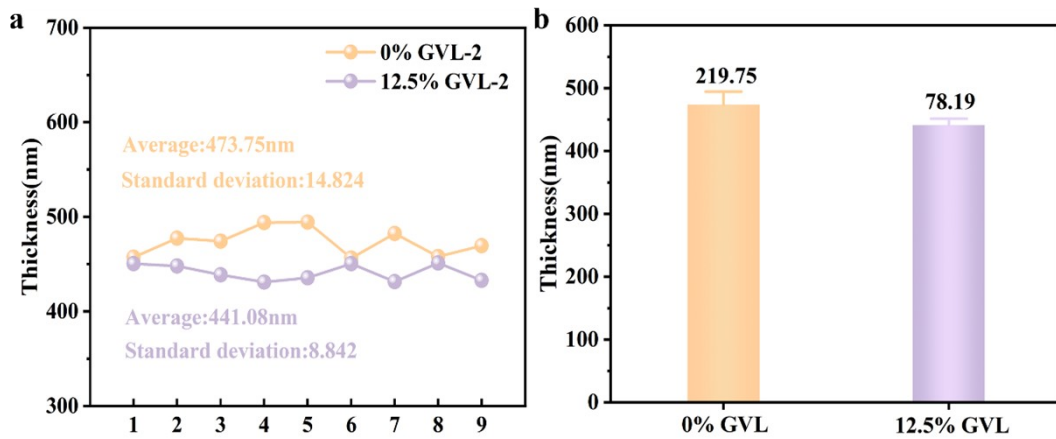


Fig. S4 (a) Statistics of over layer thickness at 9 points for 12.5% GVL and 0% GVL. (b) The variance of thickness for 12.5% GVL and 0% GVL.

Table S1. Fitting Parameters of TRPL spectra for perovskite films using biexponential decay function

	$\tau_1(\text{ns})$	$A_1(\%)$	$\tau_2(\text{ns})$	$A_2(\%)$	$T_{\text{ave}}(\text{ns})$
0% GVL	46.33	8.00	418.4	92.00	388.63
11.1% GVL	56.98	2.12	606.0	97.88	594.36
12.5% GVL	41.34	2.01	634.5	97.99	622.58
14.3% GVL	46.46	1.54	604.1	98.46	595.51

Table S2. Average and champion parameters of photovoltaic performance of 0% GVL, 14.3% GVL, 12.5% GVL, 11.1% GVL, 10.0% GVL, 12.5% DMSO and 12.5%

DMF (reverse scan)					
Sample		<i>V_{oc}</i> (V)	<i>J_{sc}</i> (mA/cm ²)	FF	PCE (%)
14.3% GVL	Champion	1.14	22.91	0.823	21.60
	Average	1.14	22.26	0.813	20.77
12.5% GVL	Champion	1.16	23.84	0.840	23.24
	Average	1.14	22.84	0.819	21.74
11.1% GVL	Champion	1.14	23.25	0.843	22.37
	Average	1.13	21.86	0.836	20.76
12.5% DMSO	Champion	1.13	22.23	0.808	20.30
	Average	1.12	22.09	0.779	19.43
12.5% DMF	Champion	1.05	23.30	0.831	20.40
	Average	1.03	23.00	0.809	19.75

References

- 1 Gaussian 16, Revision B.01, M. J. Frisch, G. W. Trucks, H. B. Schlegel, G. E. Scuseria, M. A. Robb, J. R. Cheeseman, G. Scalmani, V. Barone, G. A. Petersson, H. Nakatsuji, X. Li, M. Caricato, A. V. Marenich, J. Bloino, B. G. Janesko, R. Gomperts, B. Mennucci, H. P. Hratchian, J. V. Ortiz, A. F. Izmaylov, J. L. Sonnenberg, D. Williams-Young, F. Ding, F. Lipparini, F. Egidi, J. Goings, B. Peng, A. Petrone, T. Henderson, D. Ranasinghe, V. G. Zakrzewski, J. Gao, N. Rega, G. Zheng, W. Liang, M. Hada, M. Ehara, K. Toyota, R. Fukuda, J. Hasegawa, M. Ishida, T. Nakajima, Y. Honda, O. Kitao, H. Nakai, T. Vreven, K. Throssell, J. A. Montgomery, Jr., J. E. Peralta, F. Ogliaro, M. J. Bearpark, J. J. Heyd, E. N. Brothers, K. N. Kudin, V. N. Staroverov, T. A. Keith, R. Kobayashi, J. Normand, K. Raghavachari, A. P. Rendell, J. C. Burant, S. S. Iyengar, J. Tomasi, M. Cossi, J. M. Millam, M. Klene, C. Adamo, R. Cammi, J. W. Ochterski, R. L. Martin, K. Morokuma, O. Farkas, J. B. Foresman, and D. J. Fox, Gaussian, Inc., Wallingford CT, 2016.
- 2 M. J. Frisch, J. A. Pople, J. S. Binkley, *J. Chem. Phys.*, 1984, **80**, 3265-3269.
- 3 A. D. Becke, *J. Chem. Phys.*, 1992, **96**, 2155-2160.
- 4 S. Grimme, J. Antony, S. Ehrlich, *J. Chem. Phys.*, 2010, **132**, 154104.